Momentum-based whole-body control strategies for space robots

Workshop on **Cognitive Whole-Body Control for Compliant Robot Manipulation**

Alessandro Massimo Giordano (TUM, DLR)

1 – Classical control strategies for space robots

Fixed-Base (base rigidly controlled) $f_b \neq 0$

- High fuel expenditure ✗
- Thrusters saturation limits arm speed ✗
- Stable after contacts ✓
- Workspace can be moved in space ✓

Floating-base (base uncontrolled): free-floating $f_b = 0$

- Zero fuel consumption ✓
- Full arm speed achievable ✓
- Unstable after contacts (inertial drift) ✗
- Workspace cannot be moved in space ✗

Idea: merge advantages of both approaches by extending floating-base strategy

- Use thrusters, **but not to rigidly control the base**
- Use thrusters ***only*** to stop the drift and control the workspace

Inertial drift

- Caused by transfer of linear and angular during the contact
- Dumping of the momentum solves the problem:

*[1] A. M. Giordano et al, "**Momentum Dumping for Space Robots**", in 2017 IEEE Conference on Decision and Control (CDC).*

Workspace control

- Contact makes the workspace shift (Fig. 1)
- Control of the CoM enables workspace restore:

*[2] A. M. Giordano et al, "**Workspace fixation for free-floating robot operations**", in 2018 IEEE International Conference on Robotics and Automation (ICRA).* new

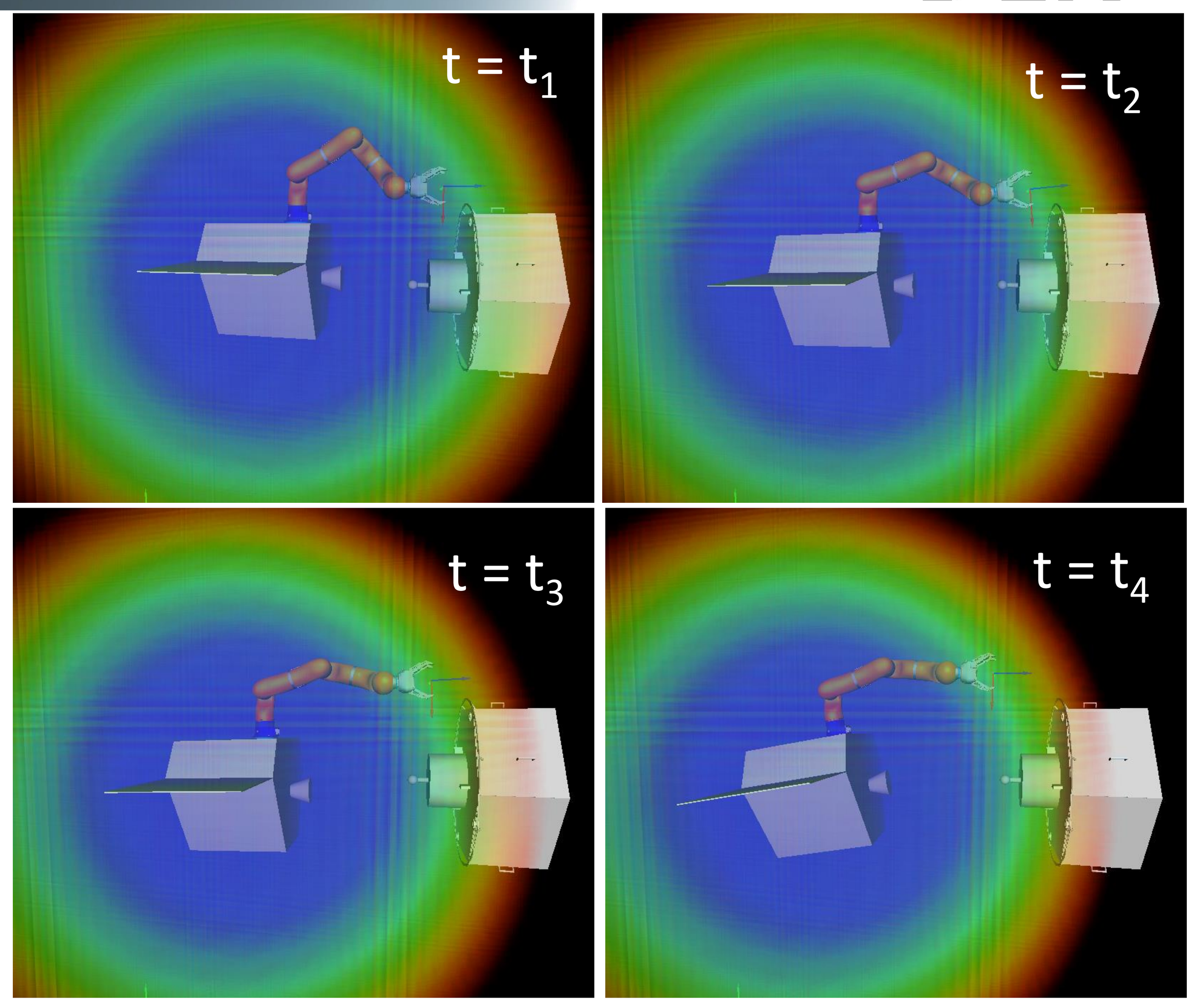

Fig. 1 – Target satellite exits the workspace when workspace is displaced due to contact

2 – External/internal end-effector motion decomposition

$$\nu_e = \underbrace{J_m^* \dot{q}}_{\nu_{e,int}} + \underbrace{A_{eb} M_b^{-1} A^T h}_{\nu_{e,lock}} \in \mathbb{R}^6$$

$\nu_{e,int} \in \mathbb{R}^6$ end-effector «internal» velocity

$\nu_{e,lock} \in \mathbb{R}^6$ end-effector «locked» velocity

$h \in \mathbb{R}^6$ momentum (linear+angular)

New task-space

CoM velocity, Angular momentum, End-effector **internal** velocity:

$$\begin{bmatrix} v_c \\ h_r \\ \nu_{e,int} \end{bmatrix} = \underbrace{\begin{bmatrix} R_{cb} & -R_{cb}[p_{bc}]^\wedge & R_{cb}\bar{J}_v \\ 0 & I_C R_{cb} & I_C R_{cb} \bar{J}_\omega \\ 0 & 0 & J_m^* \end{bmatrix}}_{\Gamma} \begin{bmatrix} v_b \\ \omega_b \\ \dot{q} \end{bmatrix}$$

Triangular task-space dynamics

External subsystem:
$$m\dot{v}_c = f_c$$
$$\dot{h}_r = \tau_c$$

Internal subsystem:
$$M_e^* \dot{\nu}_{e,int} + C_e^* \nu_{e,int} + C_{ec} v_c + C_{eh} h_r = w_{e,int}$$

3 – Controllers

Controller 1: Floating-base with momentum dumping

Net centroidal force: $f_c = -D_{h_t} h_t$ (Linear momentum dumping)

Net centroidal torque: $\tau_c = -D_{hr} h_r$ (Angular momentum dumping)

End-effector **internal** wrench: $w_{e,int} = -J_{\tilde{x}_e \nu_e}^T K_e \tilde{x}_e - D_e \nu_e$ (End-effector control)

Controller 2: Floating-base with workspace restore

$f_c = -K_c \tilde{p}_c - D_c v_c$ (CoM control)

$\tau_c = -D_{hr} h_r$ (Angular momentum dumping)

$w_{e,int} = -J_{\tilde{x}_e \nu_e}^T K_e \tilde{x}_e - D_e \nu_e$ (End-effector control)

Asymptotic stability

- Cascaded stability proof
- Continuum of equilibrium points (joints and base attitude converge to new positions)

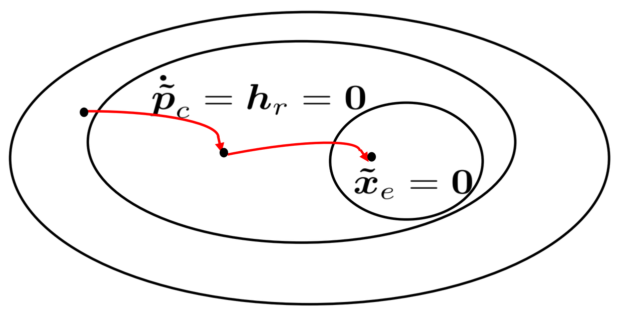

4 – Triangular actuation

Advantage 1: EE task is not executed by base actuators (**improved fuel efficiency/saturation**)

Base actuation force (thrusters), Base actuation torque (thrusters/reaction wheels), Arm joint torques:

$$\begin{bmatrix} f_b \\ \tau_b \\ \tau \end{bmatrix} = \underbrace{\begin{bmatrix} R_{cb}^T & 0 & 0 \\ [p_{bc}]^\wedge R_{cb}^T & R_{cb}^T & 0 \\ \bar{J}_v^T R_{cb}^T & \bar{J}_\omega^T R_{cb}^T & J_m^{*T} \end{bmatrix}}_{\Gamma^T} \begin{bmatrix} f_c \\ \tau_c \\ w_{e,int} \end{bmatrix}$$

Controller works nominally in **free-floating mode** (converged CoM)

$$f_b = 0$$
$$\tau_b = 0$$
$$\tau = -J_m^{*T} \left(J_{\tilde{x}\nu}^T K_e \tilde{x}_e - D_e \nu_e \right)$$

Advantage 2: Thrusters are activated automatically only to restore CoM after contact **(almost zero fuel consumption)**

5 – Experimental results

The On-Orbit Servicing Simulator (Fig. 2)

- Real arm dynamics
- Torque-controlled arm (LBR IV+)
- Simulated satellite dynamics (150kg)
- Full 6 degrees-of-freedom microgravity simulation

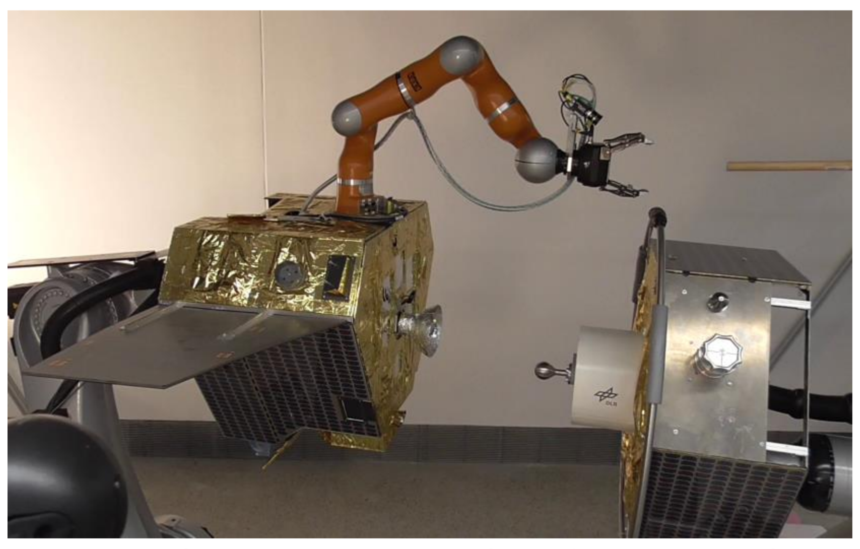

Fig. 2 –The OOS-Sim: a hardware-in-the-loop testbed for simulating space robots

Experiment

- Repeated impulses on end-effector using a stick

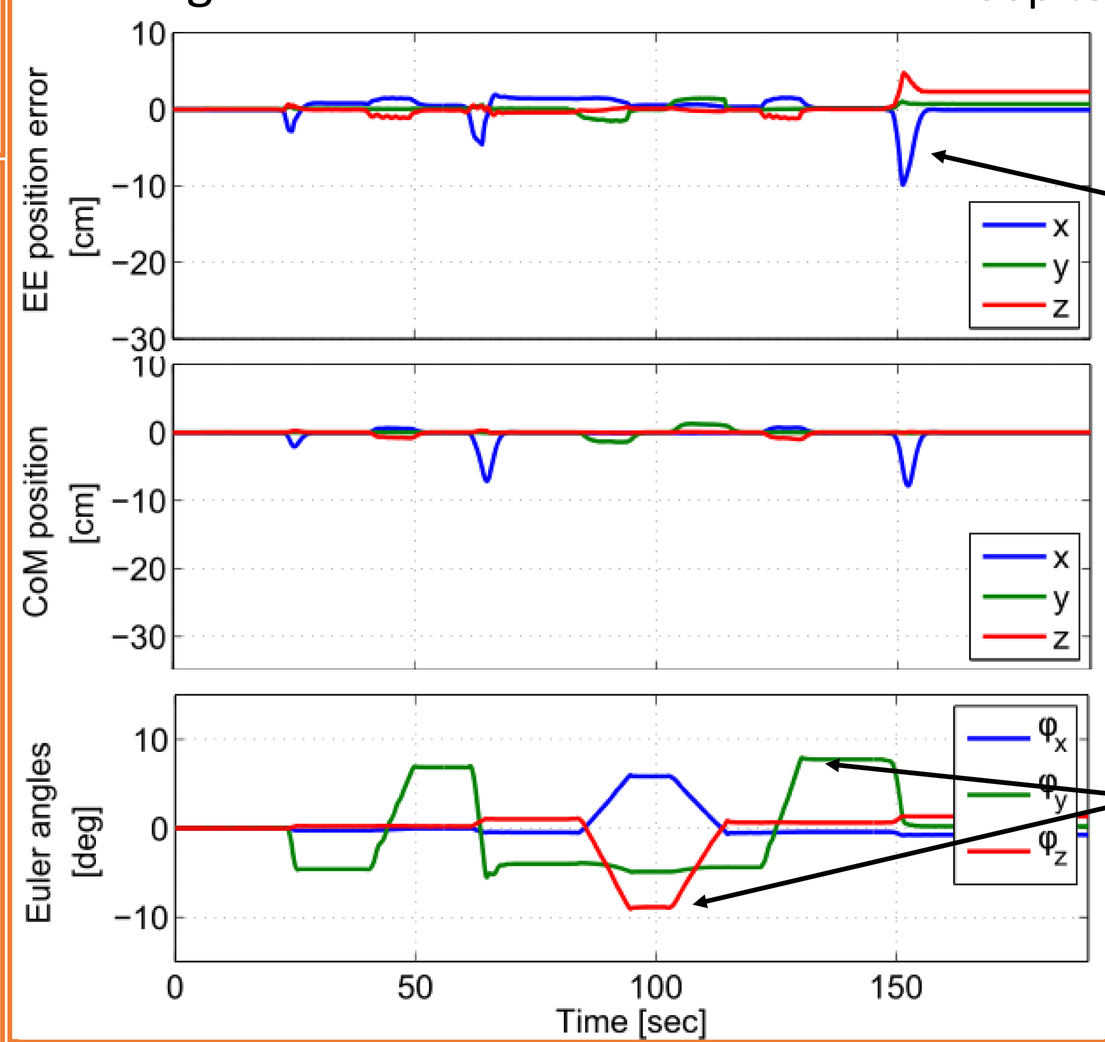

6 – State reconstruction on real system (nontumbling target)

Momentum/CoM state reconstruction $v_c, h_r, \tilde{p}_c$

	State		LIDAR p_{bt}	LIDAR v_{bt}	Star Tracker R_b	Gyro ω_b	Encod. q	Encod. $\dot{q}$
Mom. dumping	Inertial velocity of CoM	v_c		×	×	×	×	×
Mom. dumping	Total angular momentum	h_r			×	×	×	×
Workspace fixation	CoM pos. error vector	$\tilde{p}_c$	×		×		×	

End-effector state reconstruction $\tilde{x}_e, \nu_e$

- **Option 1:** in-hand stereo cameras (direct measurement)
- **Option 2:** reconstructed with forward kinematics (needs base measurements)

Sensors:

- LIDAR: 3 Hz
- Star Tracker: 3 Hz
- Gyro: 3 Hz
- Encoder: 1kHz
- In-hand cameras: 10 Hz

7 – Ongoing work

1. State reconstruction by fusion of satellite and arm sensors
2. Extension to tumbling target
3. Validation of method with pulsed thrusters.

Contact:
alessandro.giordano@dlr.de

Workshop contribution